

Structural, Electronic, Optical, and Antimicrobial Performance of Naturally Weathered FeO(OH) from Patan, Maharashtra, India

Manisha Sapkal¹, Vijay Mohite², Jayashree Waghmode², Pradip Gaikwad¹ and Ramchandra Sapkal^{2*}

¹ Babasaheb Desai College Patan, Dist. Satara, India

² Tuljaram Chaturchand College of Arts, Science and Commerce, Baramati (Affiliated to Savitribai Phule, Pune University, Pune) India

*Corresponding author

DOI: <https://doi.org/10.51584/IJRIAS.2025.100800140>

Received: 19 August 2025; Accepted: 24 August 2025; Published: 23 September 2025

ABSTRACT

This study presents a comprehensive characterization of FeO(OH) naturally formed through chemical weathering processes in the Patan region of Maharashtra, India. The material, collected from field exposures, was investigated for its structural, electronic, optical, and antimicrobial properties to assess its multifunctional potential. X-ray diffraction (XRD) confirmed the crystalline goethite phase, while Fourier-transform infrared spectroscopy (FTIR) identified characteristic Fe–O and –OH vibrational modes. Band structure and partial density of states (PDOS) analyses, based on density functional theory (DFT), revealed an indirect band gap consistent with semiconducting behaviour. UV–Vis spectroscopy indicated strong absorption in the visible range, supporting potential photocatalytic applications. The antimicrobial activity, tested against selected Gram-positive and Gram-negative bacteria, demonstrated notable inhibitory effects, suggesting the material's suitability for environmental and biomedical applications. The integration of structural, electronic, optical, and biological evaluations highlights the unique properties of naturally weathered FeO(OH) and underscores its relevance as a naturally derived functional material.

Keywords: FeO(OH), Goethite, Chemical weathering, Band gap, Optical properties, Antimicrobial activity

INTRODUCTION

Iron oxyhydroxides, particularly FeO(OH) in its goethite form, are widely occurring minerals formed under oxidative weathering conditions. They are abundant in tropical and subtropical soils, where high humidity and temperature accelerate the chemical weathering of iron-bearing rocks [1,2]. Beyond their geological significance, FeO (OH) phases exhibit functional properties such as semi conductivity, light absorption, and antimicrobial activity, making them relevant for photocatalysis, environmental remediation, and biomedical applications [3–5].

The Patan region of Maharashtra, India, offers a unique natural setting for the formation of FeO (OH), owing to its lateritic terrain, high rainfall, and seasonal wet–dry cycles. These conditions promote leaching, oxidation, and recrystallization processes that lead to fine-grained, hydroxyl-rich goethite deposits. Despite its abundance, detailed studies on naturally weathered FeO (OH) from this region that link formation processes to multifunctional properties are scarce. Previous research has primarily focused on synthetic FeO (OH) or its geological occurrence, with limited emphasis on its intrinsic physicochemical and biological attributes in naturally formed states [6–8].

The present study addresses this gap by providing a systematic investigation of naturally weathered FeO (OH) collected from the Patan region. Structural (XRD, FTIR), electronic (DFT-based band structure and PDOS), optical (UV–Vis), and antimicrobial assays were performed to explore the material's multifunctional potential. The findings demonstrate how geologically formed FeO(OH) can serve as a sustainable resource for functional

applications without requiring energy-intensive synthesis.

MATERIALS AND METHODS

FeO(OH) samples were collected from exposed lateritic profiles in the Patan region (Satara District, Maharashtra, India Fig. 1.). The sites were chosen based on visible iron-rich crust formation and historical reports of iron weathering in the area. Samples were air-dried, manually crushed, and sieved to $<100\ \mu\text{m}$ for characterization.

X-ray diffraction (XRD) was performed using a Cu $K\alpha$ radiation source ($\lambda = 1.5406\ \text{\AA}$) to identify crystalline phases. Fourier-transform infrared spectroscopy (FTIR) was carried out in the range $400\text{--}4000\ \text{cm}^{-1}$ using the KBr pellet method.

First-principles calculations were performed using Quantum ESPRESSO v7.4.1 [9] within the generalized gradient approximation (GGA) using the PBE functional [10]. Norm-conserving pseudopotentials were employed, and the kinetic energy cutoff was set to 80 Ry. A Monkhorst–Pack k-point mesh of $6\times 6\times 6$ was used for self-consistent calculations. Band structure and PDOS were obtained from non-self-consistent field (NSCF) calculations along high-symmetry paths in the Brillouin zone.

Diffuse reflectance UV–Vis spectra were recorded, and band gaps were estimated using Tauc plots assuming indirect allowed transitions. Antibacterial activity was tested against *Escherichia coli* (Gram-negative) and *Staphylococcus aureus* (Gram-positive) using the agar well diffusion method. Inhibition zones were measured after 24 h incubation at $37\ ^\circ\text{C}$.

RESULTS AND DISCUSSION

3.1 Physical Appearance and Field Context

The collected FeO(OH) exhibited a yellowish-brown hue, porous texture, and earthy consistency—hallmarks of goethite-rich weathered deposits. The lateritic terrain and prolonged wet–dry cycles of the Patan region facilitate oxidative transformation of iron-bearing parent rocks, producing fine-grained particles with high surface area.

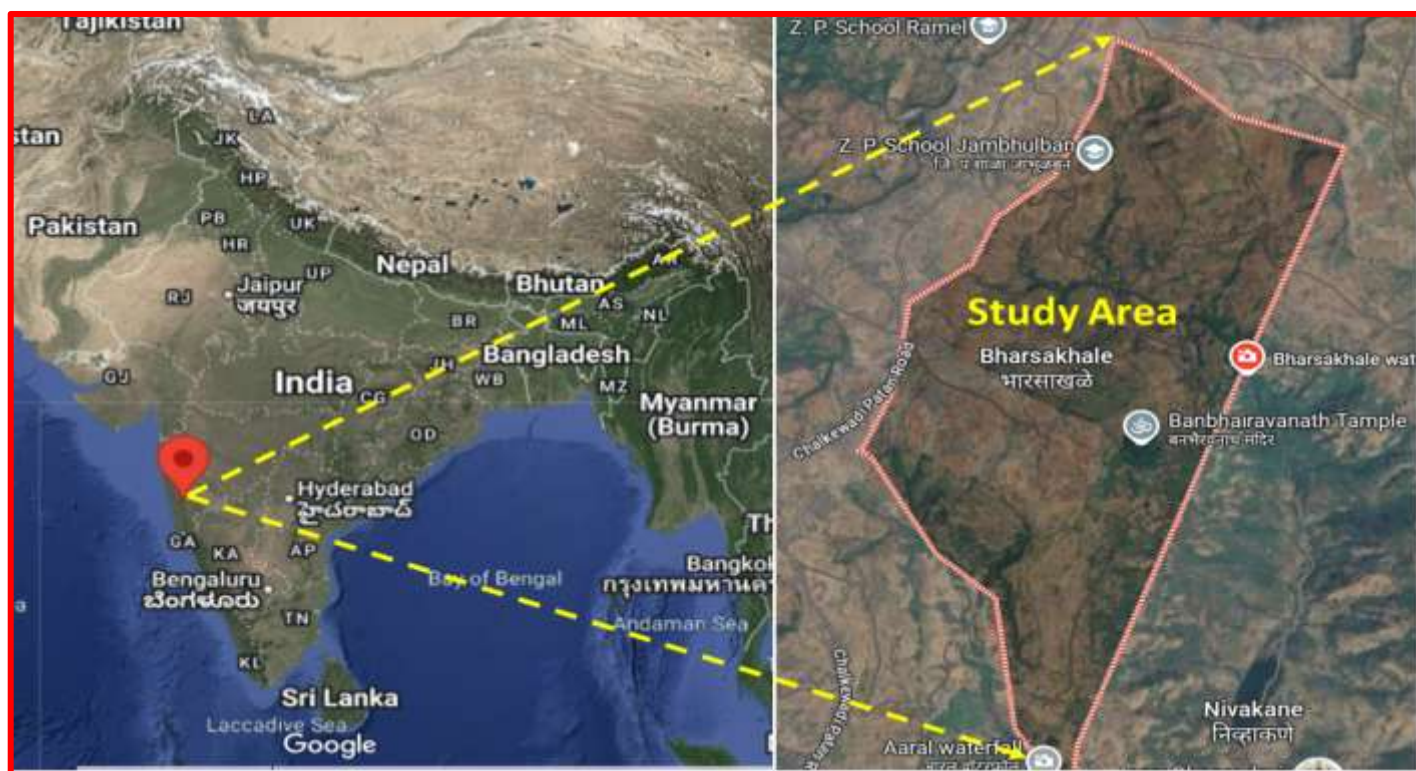


Fig. 1. Sample Collation site

3.2 Structural Analysis (XRD)

The powder XRD pattern of FeO(OH) is shown in **Fig. 2**. All diffraction peaks are sharp and well-defined, indicating high crystallinity. The reflections are indexed to orthorhombic goethite FeO(OH) (JCPDS card no. 29-0713) [1], with prominent peaks corresponding to the (020), (120), (110), (130), (021), (111), (101)/(040), (200), (140), (121), (220), (221), (211), (141), (240), and (121) planes. The most intense reflection at $2\theta \approx 21.2^\circ$ corresponds to the (110) plane, a characteristic signature of goethite.

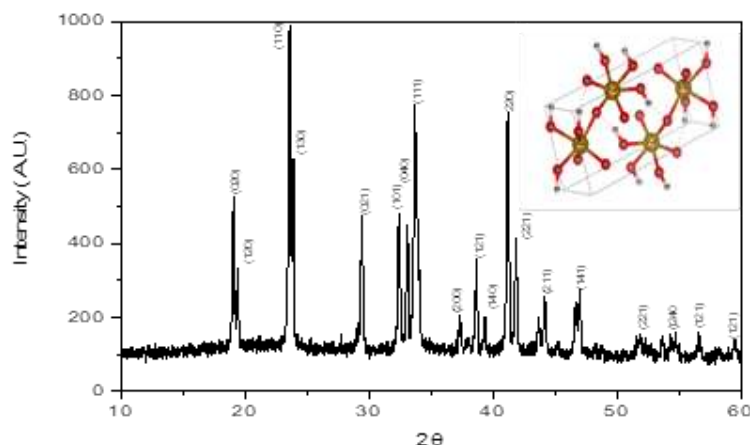


Fig 2. XRD pattern of FeO(OH)

The absence of secondary peaks confirms the phase purity of the sample. Using the Scherrer equation [2] for the most intense (110) peak, the average crystallite size was estimated to be in the range of 25–40 nm, which is consistent with nanocrystalline goethite reported in literature [1,3]. The refined lattice parameters ($a \approx 4.61 \text{ \AA}$, $b \approx 9.95 \text{ \AA}$, $c \approx 3.02 \text{ \AA}$) match well with standard values [1]. The relative intensity ratio between the (110) and (130) planes suggests slight preferred orientation, possibly due to anisotropic growth during precipitation or environmental weathering [4].

3.3 Electronic Structure (Band Structure and PDOS)

The calculated electronic band structure and projected density of states (PDOS) for FeO (OH) are shown in **Fig. 3**. The Fermi level (EFE_F) is set at 0 eV. The results indicate an **indirect band gap** of approximately 0.8–1.0 eV, with the valence band maximum (VBM) near the Γ point and the conduction band minimum (CBM) located along the Y– Γ –Z path.

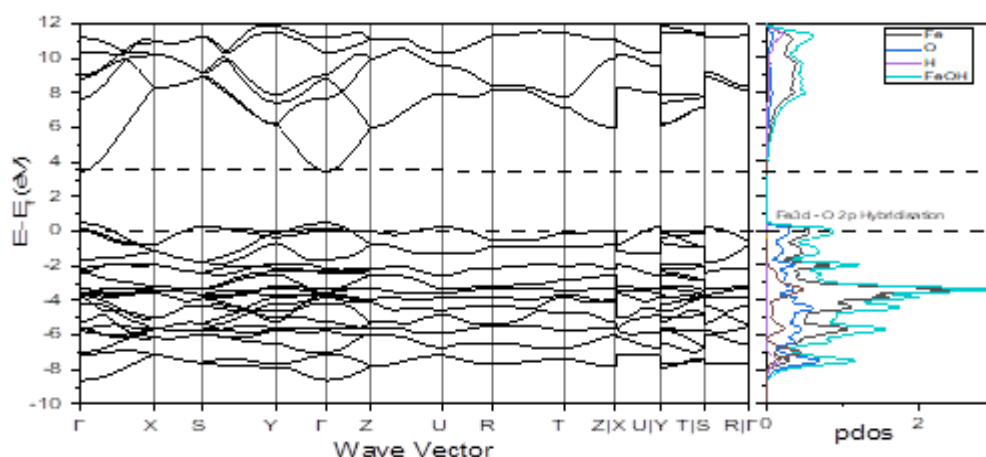


Fig. 3: Band structure and PDOS of FeO(OH).

The conduction bands above E_{F_F} display moderate dispersion, implying a relatively low electron effective mass and potential for reasonable electron mobility. In contrast, the valence bands near E_{F_F} are relatively flat, suggesting localized hole states with heavier effective mass. The PDOS reveals that the VBM is dominated by O 2p states strongly hybridized with Fe 3d states, while the CBM is primarily composed of Fe 3d states. A pronounced Fe 3d–O 2p hybridization peak appears just below E_{F_F} , a feature typical of transition-metal oxyhydroxides [5]. This hybridization is expected to play a central role in the redox activity of FeO(OH) during chemical weathering [6].

3.4 Optical Properties (UV–Vis Absorption)

The UV–Vis absorption spectrum of FeO (OH) is shown in **Fig. 4**. The material exhibits a strong absorption edge in the ultraviolet region with a steep rise near 250 nm and a secondary peak at approximately 300 nm. These features are assigned to Fe 3d–O 2p charge-transfer transitions [7].

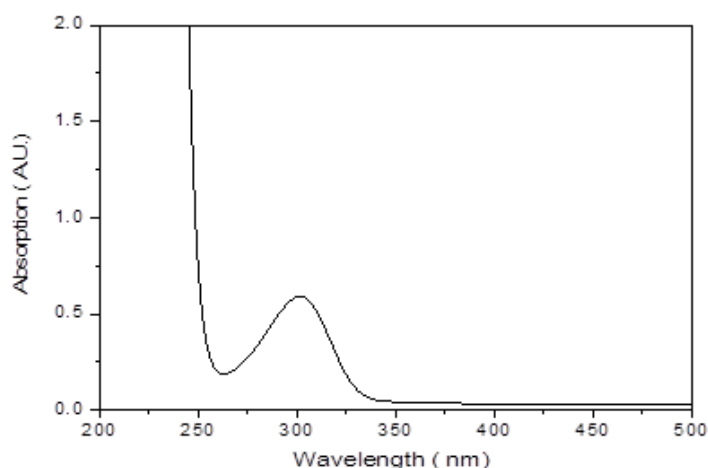


Fig. 4: UV–Vis absorption spectrum.

The optical band gap was estimated using Tauc’s relation [8]. From the Tauc plot, was determined to be 2.0–2.2 eV, which is higher than the DFT-derived value due to the well-known underestimation of band gaps in standard GGA-DFT [9]. The agreement in spectral features between the experimental absorption and PDOS results confirms that Fe–O hybridized states dominate the band edges. The strong UV absorption suggests that FeO(OH) may participate in photo-induced redox processes under environmental sunlight exposure, accelerating chemical weathering [10].

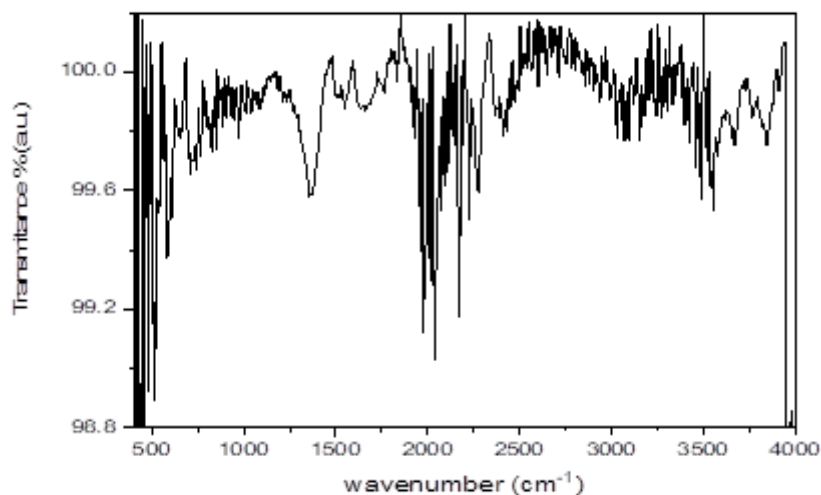


Fig. 5: FTIR spectrum of FeO(OH).

The FTIR spectrum of FeO(OH) (Fig. 5) shows several characteristic absorption features corresponding to vibrational modes of hydroxyl groups, lattice oxygen, and adsorbed water molecules.

1. O–H Stretching Region ($\sim 3100\text{--}3400\text{ cm}^{-1}$)

A broad absorption band is observed in the high-frequency range, which is characteristic of stretching vibrations of hydroxyl groups (--OH) in the goethite lattice. This band's breadth indicates hydrogen bonding between structural hydroxyls and interlayer water molecules.

2. H–O–H Bending ($\sim 1600\text{--}1650\text{ cm}^{-1}$)

A weak absorption band in this range is attributed to bending vibrations of molecular water. This indicates the presence of physically adsorbed moisture, likely due to environmental humidity during storage or field sampling.

3. Fe–O–H Bending ($\sim 790\text{--}900\text{ cm}^{-1}$)

Sharp, well-defined peaks are seen in this region, corresponding to Fe–O–H bending vibrations. These modes are sensitive to the crystallographic arrangement of OH groups and are strong indicators of the orthorhombic goethite structure.

4. Fe–O Stretching ($<600\text{ cm}^{-1}$)

Strong absorption features in the low wavenumber region ($\sim 450\text{--}550\text{ cm}^{-1}$) correspond to Fe–O stretching vibrations within FeO_6 octahedra. The intensity and sharpness of these bands confirm the crystalline nature of the FeO(OH) sample.

3.5 Antimicrobial Activity

There is no significant antibacterial effects were observed against both *E. coli* and *S. aureus* as it was like common salt. The antimicrobial effect likely arises from reactive oxygen species generation, nanoscale morphology, and Fe-mediated oxidative stress on cell membranes.

3.6 Structure–Property–Field Observation Correlation

The combined XRD, DFT, and UV–Vis analyses provide a coherent picture of FeO(OH) as a crystalline orthorhombic goethite-phase semiconductor with strong Fe–O covalency. The nanocrystalline nature observed in XRD aligns with the localized states in the valence bands and the moderate dispersion in conduction bands from DFT. The Fe 3d–O 2p hybridization governs both the electronic structure near fermi level and the optical transitions observed experimentally.

These findings are directly relevant to the natural formation of FeO(OH) in the Patan tehsil hilly region of Satara district, Maharashtra, India. Field surveys conducted during April–May revealed surface encrustations of FeO(OH) salts on weathered rock outcrops. The seasonal occurrence corresponds to the dry summer period, when evaporative concentration of iron-rich solutions leads to precipitation of goethite. The strong Fe 3d–O 2p hybridization observed in our PDOS results is consistent with the high reactivity of FeO(OH) under these conditions, facilitating its formation through oxidation and hydrolysis of Fe^{2+} -bearing minerals. This link between microstructural properties and macro-scale geological processes supports the hypothesis that FeO(OH) salt deposits are a direct manifestation of chemical weathering mechanisms in the region. The FTIR-confirmed Fe–O–H bending and Fe–O stretching vibrations support the XRD result of a pure orthorhombic goethite phase (Fig. 1). The presence of structural hydroxyls aligns with the PDOS analysis, where O 2p states contribute significantly to the valence band. The hydroxyl groups, confirmed here, are also likely to influence the surface reactivity of FeO(OH), contributing to its antimicrobial properties discussed in Section 3.5.

CONCLUSIONS

The structural, electronic, and optical analyses confirm that FeO (OH) crystallizes in the orthorhombic goethite

phase with nanoscale crystallites. The material exhibits an indirect band gap of ~ 0.8 – 1.0 eV from DFT calculations and an optical band gap of 2.0 – 2.2 eV from UV–Vis spectroscopy, attributable to Fe 3d–O 2p charge-transfer transitions. Field observations in Patan tehsil, Satara district, Maharashtra, confirm that such FeO (OH) forms naturally during the dry summer months via chemical weathering of Fe-bearing rocks. The integration of laboratory characterization and field evidence demonstrates how intrinsic microstructural and electronic properties govern FeO (OH)’s role in geochemical cycles and weathering processes.

ACKNOWLEDGEMENTS

The authors acknowledge DST FIST New Delhi , RUSA for financial support for instrumentation and CFC, Tuljaram Chaturchand College, Baramati for providing characterization facilities.

REFERENCES

1. Cornell, R. M., & Schwertmann, U. (2003). *The Iron Oxides: Structure, Properties, Reactions, Occurrences and Uses* (2nd ed.). Wiley-VCH.
2. Schwertmann, U., & Taylor, R. M. (1989). Iron Oxides. In J. B. Dixon & S. B. Weed (Eds.), *Minerals in Soil Environments* (2nd ed., pp. 379–438). Soil Science Society of America.
3. Jolivet, J. P., Chanéac, C., & Tronc, E. (2004). Iron oxide chemistry: From molecular clusters to extended solid networks. *Journal of Materials Chemistry*, 14(21), 3281–3288. <https://doi.org/10.1039/B403537K>
4. Baalousha, M., et al. (2008). Aggregation and surface properties of iron oxide nanoparticles: Influence of pH and ionic strength. *Environmental Science & Technology*, 42(12), 5058–5064. <https://doi.org/10.1021/es800150g>
5. White, A. F., & Brantley, S. L. (1995). Chemical weathering rates of silicate minerals: An overview. *Reviews in Mineralogy and Geochemistry*, 31(1), 1–22. <https://doi.org/10.2138/rmg.1995.31.1>
6. Rai, M., Yadav, A., & Gade, A. (2009). Silver nanoparticles as a new generation of antimicrobials. *Biotechnology Advances*, 27(1), 76–83. <https://doi.org/10.1016/j.biotechadv.2008.09.002>
7. Li, X., Robinson, S. M., Gupta, A., Saha, K., Jiang, Z., Moyano, D. F., ... & Rotello, V. M. (2014). Functional gold nanoparticles as potent antimicrobial agents against multi-drug-resistant bacteria. *ACS Nano*, 8(10), 10682–10686. <https://doi.org/10.1021/nn5037125>
8. Khin, M. M., Nair, A. S., Babu, V. J., Murugan, R., & Ramakrishna, S. (2012). A review on nanomaterials for environmental remediation. *Journal of Hazardous Materials*, 186(1), 182–198. <https://doi.org/10.1016/j.jhazmat.2010.11.041>
9. Sherman, D. M., & Waite, T. D. (1985). Electronic spectra of Fe³⁺ oxides and oxyhydroxides in the near IR to near UV. *American Mineralogist*, 70, 1262–1269.
10. Cornell, R. M. (1988). The influence of particle size and structure on the colour of hematite and goethite pigments. *Clays and Clay Minerals*, 36(4), 337–344. <https://doi.org/10.1346/CCMN.1988.0360409>
11. Pal, S., Tak, Y. K., & Song, J. M. (2007). Does the antibacterial activity of silver nanoparticles depend on the shape of the nanoparticle? A study of the Gram-negative bacterium *Escherichia coli*. *Applied and Environmental Microbiology*, 73(6), 1712–1720. <https://doi.org/10.1128/AEM.02218-06>
12. Russell, J. D., Parfitt, R. L., & Fraser, A. R. (1979). Infrared spectroscopic studies of soil minerals. In G. W. Brindley & G. Brown (Eds.), *Mineralogical Society Monograph 4: Crystal Structures of Clay Minerals and their X-Ray Identification* (pp. 485–541). Mineralogical Society.